



## Investigation of the adsorption behavior of glycine peptides on 12% cross-linked agarose gel media

Xiaoou Zhang<sup>a</sup>, Jörgen Samuelsson<sup>b</sup>, Jan-Christer Janson<sup>b</sup>, Changhai Wang<sup>a</sup>, Zhiguo Su<sup>c</sup>, Ming Gu<sup>c</sup>, Torgny Fornstedt<sup>b,\*</sup>

<sup>a</sup> Department of Biological Science and Technology, School of Environmental and Biological Science and Technology, Dalian University of Technology, Dalian, 116024, China

<sup>b</sup> Department of Physical and Analytical Chemistry, Uppsala Biomedical Centre, Uppsala University, Box 599, SE-751 24 Uppsala, Sweden

<sup>c</sup> National Key Laboratory of Biochemical Engineering, Institute of Process Engineering, Chinese Academy of Sciences, Box 353, Beijing, 100190, China

### ARTICLE INFO

#### Article history:

Received 29 April 2009

Received in revised form 2 December 2009

Accepted 18 January 2010

Available online 25 January 2010

#### Keywords:

Superose 12 10/300 GL

Peptides

Adsorption isotherms

Adsorption energy distribution

Heterogeneous interaction

Hydrogen bond formation

Langmuir model

Tóth model

bi-Langmuir model

Mixed mode

Electrostatic interactions

### ABSTRACT

The highly cross-linked 12% agarose gel Superose 12 10/300 GL causes retardation of glycine peptides when mobile phases containing varying concentrations of acetonitrile in water are used. An investigation has been made into the retention mechanism behind this retardation using the glycine dipeptide (GG) and tripeptide (GGG) as models. The dependence of retention times of analytical-size peaks under different experimental conditions was interpreted such that the adsorption most probably was caused by the formation of hydrogen bonds but that electrostatic interactions cannot be ruled out. Thereafter, a nonlinear adsorption study was undertaken at different acetonitrile content in the eluent, using the elution by characteristic points (ECPs) method on strongly overloaded GG and GGG peaks. With a new evaluation tool, the adsorption energy distribution (AED) could be calculated prior to the model selection. These calculations revealed that when the acetonitrile content in the eluent was varied from 0% to 20% the interactions turned from (i) being homogenous (GG) or mildly heterogeneous (GGG), (ii) via a more or less stronger degree of heterogeneity around one site to (iii) finally a typical bimodal energy interaction comprising of two sites (GG at 20% and GGG at 10% and 20%). The Langmuir, Tóth and bi-Langmuir models described these interesting adsorption trends excellently. Thus, the retardation observed for these glycine peptides is interpreted as being of mixed-mode character composed of electrostatic bonds and hydrogen bonds.

© 2010 Elsevier B.V. All rights reserved.

### 1. Introduction

The highly cross-linked 12% agarose gel Superose 12 10/300 GL (originally named Superose 12 HR 10/30) was introduced in 1982 as a size exclusion chromatography media for proteins and other water soluble high molecular compounds. However, early studies revealed that the product displayed hydrophobic adsorption of low molecular weight amphiphilic substances such as long chain alcohols [1]. The media is manufactured using an extensive cross-linking procedure [2,3] based on reactions with a combination of long and short chain aliphatic bis-epoxides. The cross-linkers react with hydroxyl groups of the galactosyl residues of the agarose gel matrix as well as with those hydroxyls belonging to the cross-linkers already generated in the initial cross-linking reaction. Thus, a variety of polar groups, primarily ether bonds but also primary and secondary alcohol hydroxyl groups and hemiacetal groups,

as well as hydrophobic butanediol moiety residues, are introduced into the agarose gel during the cross-linking reactions. The polar groups primarily provide hydrogen bond acceptor functions, and form the primary interaction sites for hydrogen bond donor molecules, such as polyphenols in the presence of acetonitrile. Likewise, the long aliphatic hydrocarbon chains, created by the cross-linking reaction with butanediol diglycidyl ether, would provide hydrophobic interaction sites in the presence of water.

Recent studies have shown that Superose 12 10/300 GL functions as a mixed-mode adsorption media for low molecular weight substances such as polyphenols and other active components in traditional Chinese medicine [4–8]. As with other mixed-mode media [9] the adsorption characteristics are dependent on the composition of the mobile phase. Thus, in the presence of pure water, hydrophobic interactions prevail whereas in the presence of pure acetonitrile the retardation is primarily based on hydrogen bond formation with the surface structures of Superose 12 acting as hydrogen bond acceptors. This mixed-mode adsorption was convincingly exemplified by plotting the retention factor of the polyphenolic compound (–)-epigallocatechin gallate versus the percent acetonitrile content in the mobile phase (acetonitrile)/Milli-

\* Corresponding author. Fax: +46 18 471 3692.

E-mail address: [torgny.fornstedt@ytbioteknik.uu.se](mailto:torgny.fornstedt@ytbioteknik.uu.se) (T. Fornstedt).

Q water) going from 20% to 95% acetonitrile. An U-shaped curve was obtained (see Fig. 7 in ref. [4]) with a minimum retardation at around 60% acetonitrile indicating a hydrophobic adsorption at low acetonitrile content and a hydrogen bond adsorption mechanism at high acetonitrile content.

In recent years there has been an increased interest in using hydrophilic interaction chromatography (HILIC) [9–11] based on polar stationary phases combined with partly aqueous eluents (around 5–40% water in acetonitrile). The retention mechanism of the HILIC phases makes them especially useful for separations of peptides and other polar organic compounds as a complement to reversed phase chromatography for these types of solutes. The highly hydrophilic character of the Superose 12 gel triggered an interest in investigating if the Superose 12 gel would possess selectivity properties for peptides similar to that of known HILIC phases. To this end it was decided to start the investigation by performing a deeper study of the adsorption mechanism of the interactions between simple glycine peptides and the Superose 12 gel.

Recently, modern computers have made it possible to simulate chromatographic band profiles for process optimization [12]. The main prerequisite for the computer simulations are adsorption isotherms [13]. An adsorption isotherm is a function that describes the relationship of the solute's concentration in the mobile and stationary phase at a specific and constant column temperature (isothermal conditions). The most common type of adsorption isotherm (type I) has a convex shape. Several different adsorption isotherm models have been suggested to describe the extremely varied adsorption behavior for different solute–phase separation systems. The simplest adsorption model is the Langmuir assuming a single adsorption site, i.e. all molecules interact with identical adsorption energy and a monolayer adsorption. However, the Langmuir model is often unsuccessful to describe the partitioning, because solutes often participate in many different types of interactions (e.g. electrostatic, hydrophobic etcetera) with a surface. Therefore, often other models are required.

Adsorption isotherms are very important for a deeper understanding of the adsorption process and of the retention mechanism. Traditionally, retention mechanisms are interpreted based on retention times of analytical-size peaks, i.e. peaks obtained after the injection of small amounts of solute. From these retention times traditional distribution coefficients are calculated, i.e. coefficients related to the slope of the adsorption isotherm at low concentrations. However, these equilibrium constants are lumped and cannot resolve the different adsorption sites often prevailing in a multi-phase system. Therefore, the lumped constants often result in incorrect conclusions of single-site bindings, although, in reality the interactions may involve several different adsorption sites with completely different adsorption properties [14,15]. However, by instead determining the adsorption isotherms of the actual phase system, i.e. the relation between the solute concentrations adsorbed to the stationary phase and the mobile phase concentration, with an as wide concentration range as possible, a complete census of all interactions in the actual process can be obtained.

A considerable number of experimental methods have been suggested to account for the liquid–solid equilibrium data [12]. One of the most accurate techniques is frontal analysis (FA). However, the FA method is tedious and time-consuming and also consumes large amounts of solute. The elution by characteristic point (ECP) method is much faster and consumes less solute which is why it is more suitable for life science studies. In the ECP method, the adsorption isotherm data points are simply generated from the diffusive part of an overloaded elution profile [12].

A firm two-step evaluation approach [16,17] was recently suggested for adsorption data prior to the traditional model selection process of best fitting. First, (i) classical Scatchard plots are used to make a preliminary selection of the type of adsorption isotherm.

Thereafter, (ii) the degree of heterogeneity of the phase system is determined by calculation of the adsorption energy distribution (AED). The purpose of the combined use of classical Scatchard plots and AED calculations is to narrow down the number of possible adsorption models to only a few, before a model is selected. Finally, proper adsorption isotherm models, as predicted by the two prior steps, are fitted to the experimental adsorption isotherms and statistically evaluated.

The aim of this study is to investigate and characterize the interactions between selected model peptides and the gel Superose 12, using the theory of nonlinear chromatography in combination with the above mentioned approach.

## 2. Theory

### 2.1. Determination of adsorption isotherms

It is possible to measure the adsorption isotherm ( $q(C)$ ) from the diffusive part of a profile; the method is called “elution by characteristic points”. When integrating the diffuse tail of a large overloaded profile for a type I adsorption isotherm (convex adsorption isotherm) we obtain:

$$q(C) = \frac{1}{V_a} \int_0^C (V_R(C) - V_0 - V_{inj}) dC, \quad (1)$$

where  $V_{inj}$  is the injected volume and  $V_R(C)$  is the elution volume corresponding to mobile phase concentration  $C$ . The ECP method is derived using the ideal model and is therefore only suited for efficient systems. Therefore, the ECP method requires a separation system with high column efficiency in order to minimize the error in the determination. A plate number ( $N$ ) higher than 2000 is required for obtaining a homogenous Langmuir adsorption isotherm interaction [18] and an  $N$  higher than 5000 for a heterogeneous bi-Langmuir [19]. The efficiency of the column used in this investigation was around 9000 theoretical plates (see Table 1).

### 2.2. Adsorption isotherm

The Langmuir adsorption isotherm is the simplest nonlinear adsorption isotherm describing a finite amount of equal adsorption sites with monolayer coverage [12,20]:

$$q = \frac{q_s K C}{1 + K C} = \frac{a C}{1 + K C} \quad (2)$$

where  $q_s$  and  $K$  are the column's monolayer saturation capacity and association equilibrium constant, respectively. The distribution coefficient, or Henry constant, ( $a$ ), is the equilibrium ratio at infinite dilution of the solute; i.e. the initial slope of the adsorption isotherm. The association equilibrium constant shows an exponential relationship with the adsorption energy:

$$K = K_0 e^{(\varepsilon/RT)}, \quad (3)$$

where  $\varepsilon$  is the adsorption energy,  $R$  is the universal gas constant and  $K_0$  is the pre-exponential factor. Thus, the adsorption energy is proportional to  $\ln K$ .

**Table 1**  
Chromatographic operational conditions.

Column total volume	23.72 mL (302 mm × 10 mm)
Column hold-up volume	20.80 mL
Flow rate	0.50 mL/min
Column efficiency GG	8982 (number of plates per column)
Column efficiency GGG	9173 (number of plates per column)
Porosity	0.88

The bi-Langmuir adsorption isotherm is an expansion of the Langmuir model assuming two independent adsorption sites:

$$q = \frac{q_{s,1}K_1C}{1+K_1C} + \frac{q_{s,2}K_2C}{1+K_2C} = \frac{a_1C}{1+K_1C} + \frac{a_2C}{1+K_2C}, \quad (4)$$

where  $q_{s,i}$ ,  $a_i$  and  $K_i$  are the column's monolayer saturation capacity, association equilibrium constant and distribution coefficient for the  $i$ th adsorption site, respectively. The adsorption energy distribution is bimodal with two homogeneous sites located at adsorption energy corresponding to  $K_1$  and  $K_2$ . The bi-Langmuir model has successfully been used to describe the adsorption of enantiomers to protein stationary phases, e.g.  $\alpha_1$ -acid glycoprotein (AGP) [21]. In such cases, the adsorption process comprises of two different types of sites, one enantio-selective and one non-selective. The non-selective sites have a large capacity but low adsorption energy representing many different adsorption sites of similar energy-level all over the surface while the enantio-selective sites have low capacity but high adsorption energy and could be the active site of a protein. The bi-Langmuir model has also successfully been used to describe the adsorption of charged [22] and uncharged solutes (like phenol) on reversed phase systems (ODS columns) [23].

The Tóth adsorption isotherm is a one-site adsorption model that has a unimodal heterogeneous adsorption energy distribution, and therefore accounts well for some energetically heterogeneous surfaces:

$$q = \frac{aC}{(1+(KC)^\nu)^{1/\nu}} \quad (5)$$

where  $a$ ,  $K$  and  $\nu$  are adsorption isotherm parameters and  $\nu$  is a measurement of the heterogeneity. If  $\nu = 1$  the model becomes the Langmuir model.

### 2.3. Adsorption energy distribution (AED)

Most partitioning is energetically heterogeneous; therefore the theory should be able to handle this. The Langmuir adsorption isotherm model can be extended to a continuous distribution of independent homogeneous sites across a certain range of adsorption energies:

$$q(C) = \int_{K_{\min}}^{K_{\max}} f(\ln K)\theta(C, K)d \ln K, \quad (6)$$

where  $\theta(C, K)$  is the local adsorption model (usually the Langmuir or Jovanovic model is used) and  $f(\ln K)$  is the AED.  $K_{\min}$  and  $K_{\max}$  are governed by  $1/C_{\max}$  and  $1/C_{\min}$ , respectively, where  $C_{\min}$  and  $C_{\max}$  are the lowest and highest mobile phase concentrations measured in the adsorption isotherm [24].

The AED can be solved using many different methods, the method used in this study is the expectation maximization method [25] where the integral equation is discretized to a sum and solved in an iterative manner. Over-iteration produces noise throughout the distribution and under-iteration can lead to unconverted energy sites [23].

## 3. Experimental

### 3.1. Equipment

A Shimadzu 10Avp chromatographic system from Shimadzu corporation (Kyoto, Japan) equipped with a binary LC-10ATvp pump and a SPD-10Avp UV-detector was used. A Superose™ 12 10/300 GL column (10 mm × 302 mm; 10  $\mu$ m average particle diameter) from GE Healthcare Bio-sciences AB (Uppsala, Sweden) was temperature-controlled (using a DSHZ-300A water bath

(Taicang, Jiangsu, China). The column temperature was kept at 25.0 °C if not mentioned otherwise. A 420A plus pH meter from Thermo Fisher Scientific Inc. (Waltham, MA, USA) was used to monitor the pH value of mobile phase and sample solution.

### 3.2. Chemicals

The solutes: glycine dipeptide (GG, 99%) and glycine tripeptide (GGG, 99%) were obtained from Sigma–Aldrich. The organic modifier was acetonitrile (HPLC grade) from Caledon Laboratories Ltd. (Georgetown, Ontario, Canada). The water was from a Milli-Q water purification system ZLXS 5005Y from Millipore (Molsheim, France). All the other reagents, including sodium hydroxide (NaOH), acetic acid (HAc), urea, phosphoric acid (H<sub>3</sub>PO<sub>4</sub>), sodium dihydrogen phosphate (NaH<sub>2</sub>PO<sub>4</sub>), disodium hydrogen phosphate (Na<sub>2</sub>HPO<sub>4</sub>), trisodium phosphate (Na<sub>3</sub>PO<sub>4</sub>), ethanol and acetone, were of analytical grade.

### 3.3. Preparation of mobile phases and samples

The mobile phases were prepared by mixing acetonitrile and Milli-Q water or phosphate buffer (ionic strength of 8 mM at pH 3, 7 and 12) in various proportions. In order to keep the same ionic strength the total phosphate buffer concentrations were 10, 5.0 and 2.1 mM at pH 3, 7 and 12, respectively. All mobile phases were passed through a 0.45  $\mu$ m filter and degassed by ultrasonication before use. All samples were dissolved in the actual mobile phase and pre-filtered using a 0.22  $\mu$ m filter to remove possible particles before injection into the chromatographic column.

#### 3.3.1. Experimental procedures – operational parameters

All experiments were performed at a constant flow rate of 0.50 mL/min. The whole column was submerged in a water bath. The media was regenerated after every peptide separation cycle by washing with 25 mL 0.5 M NaOH followed by 50 mL Milli-Q water, 25 mL 20% (v/v) HAc and 20% (v/v) ethanol water solution and finally by 150 mL Milli-Q water. Before the next run, the column was equilibrated with 5 column volumes of the actual mobile phase. The column efficiency ( $N$ ) was determined after injecting duplicates of 20  $\mu$ L of a mixture of GG and GGG (50  $\mu$ g/mL of each, monitored at 215 nm) using a mobile phase of acetonitrile/Milli-Q water (1/9, v/v). The efficiency was calculated using the width at half height method, resulting in an  $H$  of approximately three particle diameters (see Table 1). The void volume was determined after triplicate injections of 200- $\mu$ L sample 1% (v/v) acetone in the selected eluent and monitored at 280 nm.

The calibration curves were produced after injecting 500  $\mu$ L of different sample concentrations directly into the UV monitor at 222 nm; a number of 10 concentration levels were used between 1.00  $\mu$ g/mL and 1.00 mg/mL of GG or GGG peptide dissolved in the mobile phase. The UV-detector response to concentration (g/L) was fitted to a third degree polynomial.

#### 3.3.2. Experimental procedures – data collection

**3.3.2.1. Analytical study.** In all analytical investigations, 20  $\mu$ L of a sample containing a mixture of GG and GGG (50  $\mu$ g/mL of each) were dissolved in the desired eluent. The peaks were detected at 215 nm. At each mobile phase composition, or at each temperature level, the void volume was determined according to the procedure mentioned above.

The dependence of the retention time on the acetonitrile concentration in the eluent was investigated by using eluents containing different proportions of acetonitrile in Milli-Q water (0–40%, v/v). The temperature dependency was investigated using an eluent containing 10% (v/v) acetonitrile/Milli-Q water at thermo stated column temperatures of 15, 25 and 45 °C. The retention time

was also investigated by using phosphate buffer (pH 3, 7, and 12, ionic strength 8 mM).

**3.3.2.2. Adsorption study.** For this study, heavily overloaded sample injections were made into the column using an eluent containing 0%, 10% and 20% (v/v) acetonitrile in Milli-Q water. Two separate 500  $\mu$ L injections were made of 5.00 mg/mL GG/GGG for all eluents except for 15% acetonitrile were 6.00 of GG and GGG were used, respectively, and for 20% acetonitrile were 6.00 and 8.00 mg/mL were used of GG and GGG, respectively. The detector wavelength (222 nm) was not changed and the monitor was not switched off until all experiments were completed. The reason for this precaution is that a proper determination of adsorption data using the ECP method requires exact concentration data points, and the absorbance setting of a mechanistic detector can never be exactly restored (in contrast to a diode-array detector).

#### 3.4. Calculation procedures

The adsorption isotherms were determined using the ECPs method [18,19]. Before the selection of a proper adsorption isotherm model, the raw adsorption isotherm data were analyzed using a new two-step evaluation process [16,17]. First, (i) Scatchard plots were plotted ( $q$  versus  $q/C$ ) then (ii) calculations were made of the AED. Finally the model fitting was made to the most probable adsorption isotherm model – predicted by the combined analysis of steps i and ii – by a standard nonlinear least squares method [12] using the Levenberg–Marquardt algorithm as implemented in Matlab (Mathworks Inc., Natick, MA, USA).

## 4. Results and discussion

At first, an investigation was undertaken based on analytical-size retention data aimed at study the character of the binding between the glycine peptides and the Superose 12 10/300 GL gel. Thereafter, a deeper adsorption study was performed over a wider concentration range in order to obtain a quantitative determination of all possible interactions between the peptides and the gel. Table 1 shows the determined operational parameters for the system, used in the analytical as well as in the adsorption study.

#### 4.1. Analytical study

In the analytical investigation the dependence of the retention factors of the model peptides on the most important experimental conditions were investigated. The experimental factors varied were (i) the mobile phase content of the organic modifier (ii) pH and the salt/buffer concentration in the mobile phase and (iii) the phase system temperature.

##### 4.1.1. Effects of varied acetonitrile content in the mobile phase

It was recently reported that the retention times for polyphenolic substances on Superose 12 10/300 GL is strongly dependent on the acetonitrile fraction in the eluent [4–9]. When  $\log k$  (retention factor) was plotted versus the acetonitrile content, a U-shaped relation appeared with a minimum retardation at 60% acetonitrile. Further increase in the acetonitrile content caused further increase in the retention [4]. This indicates that the adsorption of

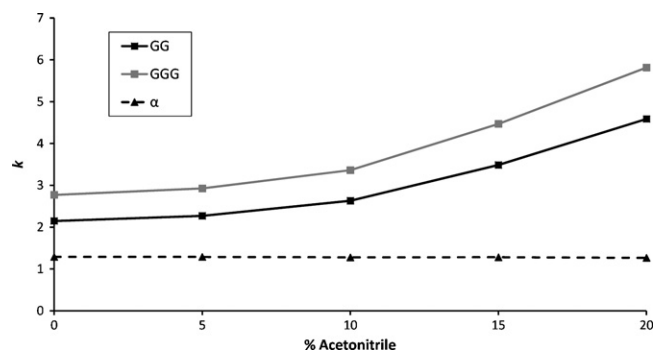


**Fig. 1.** Retention factors ( $k$ ) and selectivity factors ( $\alpha$ ) of GG and GGG for different volume fractions of acetonitrile in the eluent. 20  $\mu$ L samples of GG and GGG (0.050 mg/mL of each) were injected. For other experimental conditions see Section 3.

the polyphenolic compounds possesses a mixed-mode character. Thus hydrophobic interactions prevail at low acetonitrile concentrations whereas the formation of hydrogen bonds dominates at high modifier concentrations in line with HILIC separation principles [10,11].

The dependence of the peptide retention factor on the acetonitrile content in the mobile phase was investigated. Analytical amounts of GG and GGG were injected using eluents containing 0–40% of acetonitrile. In Fig. 1 the resulting retention factors ( $k$ ) versus the percentage of acetonitrile in the eluent were plotted. The retention factors for both GG and GGG increased dramatically with increasing acetonitrile content in the eluent (cf. Fig. 1). The highest acetonitrile concentration studied was 20% resulting in a retention factor around 5. At 40% acetonitrile the retention of GG and GGG exceeded 40 column volumes ( $k > 50$ ) suggesting even stronger retention at higher acetonitrile concentrations. Note that the selectivity ( $\alpha$ ) between GG and GGG is unchanged (see Fig. 1). Thus, in contrast to the case of polyphenols as solutes [4], the interaction between the peptides and Superose 12 10/300 GL seem not to be dominated by hydrophobic interactions at low levels of acetonitrile. This indicates that some kind of polar bonding, like hydrogen bond formations, or electrostatic interactions, could be the cause of adsorption. However, in contrast to polyphenols, the peptide retention increases even at lower acetonitrile concentrations in the eluent.

##### 4.1.2. Effects of varied pH and salt/buffer concentrations in the mobile phase

To further investigate the character of the polar binding, urea and sodium chloride were separately added to the eluent composed of Milli-Q water/acetonitrile (1/9, v/v). As urea is a neutral polar component, any decrease in retention volume of the peptide peaks is expected to be caused by hydrogen bond competition rather than suppression of electrostatic interactions. As shown in Table 2, in the absence of urea the retention volumes of GG and GGG were 76.9 and 93.3 mL, respectively. In the presence of 1 M urea the retention volumes had decreased to 29.0 and 31.6 mL, respectively. When 2 M urea was added to the mobile phase, GG and GGG eluted together and only one peak appeared at 19.7 mL; this volume is smaller than the column hold-up volume (20.4 mL)

**Table 2**  
Effects on peptide retention volume of additions of urea to the eluent.

Urea concentration (M)	GG Retention volume (mL)	GGG Retention volume (mL)	Acetone retention volume (mL)
0 (Milli-Q water)	76.91	93.29	20.58
1	28.97	31.61	20.44
2	19.68	19.68	20.37



indicating a total suppression of the adsorption. When sodium chloride (10 mM) was added to the eluent the retention of GG and GGG decreased to 18.7 mL, which is even more below the determined void volume. Thus, one cannot rule out electrostatic interactions as responsible for the retention as well (see Section 4.3).

The investigation was completed with a pH study. At first, eluents were used comprising of 20 or 50 mM buffer/acetonitrile (1/9, v/v) at pH 5, 6 and 7 (acetate was used at pH 5 and phosphate at pH 6 and 7). It was found that the peptide retention volumes were even lower as compared to the void volume (between 18.1 and 18.4 mL). As shown above (*cf.* Fig. 1), the peptide retention has a very strong but inversely relation to the water content; the lower the water contents in the eluent the stronger the peptide adsorption. We therefore tried to conduct a pH investigation using a higher amount of acetonitrile while also keeping the ionic strength as low as possible. For this purpose, eluents were used comprising of low-ionic strength phosphate buffer ( $I = 8.0$  mM)/acetonitrile mixtures of (3/7, v/v) and even (5/5, v/v) at pH 3, 7 and 12. But even at these quite promoting conditions for adsorption the peptide retentions remained negligible, except for pH 3 where a slight retention of the peptides was achieved, using buffer/acetonitrile (5/5, v/v) as eluent.

To conclude, hydrogen bonding is probably the main contribution, since it can be weakened by both urea and NaCl additions. It is clear that the adsorption is strongly counteracted by charged salt components which is why it was impossible to investigate any pH effects using eluents with 10% acetonitrile while maintaining a good buffer capacity.

#### 4.1.3. Effects of varied phase system temperature

Next, the dependence of the peptide retention factor on the column temperature was investigated. Analytical-size injections were made of GG and GGG using the eluent composed of Milli-Q water/acetonitrile (1/9, v/v) at column temperatures between 5.0 and 45.0 °C. Fig. 2 shows the van't Hoff plots for the retention factors ( $k$ ) of GG and GGG, respectively. The symbols are the experimental data and the lines the best linear fits. The slopes of the lines demonstrate that the global adsorption processes of both peptides are endothermic. The values of the adsorption enthalpy  $\Delta H$  is derived from the slope of the van't Hoff plots using the classical equation; the values were very similar for the two peptides, +3.08

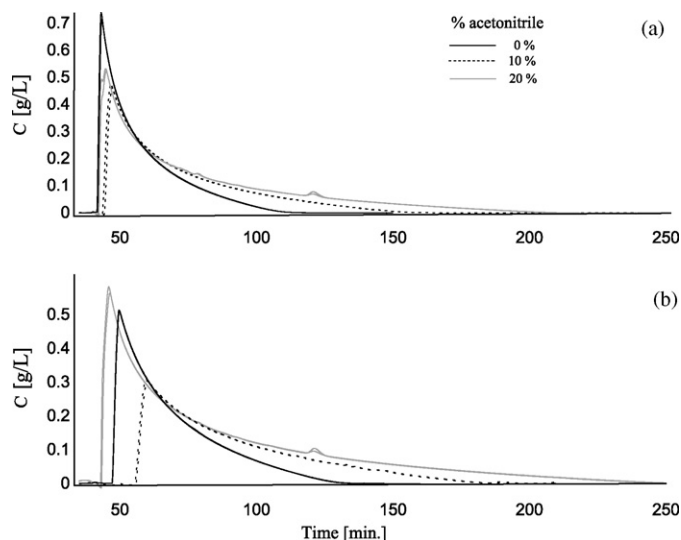


**Fig. 3.** The figure shows overlaid chromatograms for 500- $\mu$ L duplicate injections of 5 mg/mL of (a) GG and (b) GGG for all eluents except 20% acetonitrile were 6 mg/mL of GG or 8 mg/mL GGG. The acetonitrile content in the eluent was 0% (black line) 10% (dashed line) and 20% (gray line.). For other experimental conditions see Section 3.

and +3.09  $\text{kJ mol}^{-1}$  for GG and GGG, respectively. This is already indicated by the very similar slopes of the two lines in Fig. 2 and the consequence from a practical viewpoint is that the selectivity between the peptides can never be modified by changing the column temperature. The values of the adsorption entropy  $\Delta S$  were +17.2 and +19.4  $\text{mol}^{-1} \text{K}^{-1}$  for GG and GGG, respectively.

Endothermic adsorption behaviors are rather rare in chromatography and strengthen the hypothesis of polar interactions, by hydrogen bonding. In a recent publication, where the dielectric constants of acetonitrile/water mixtures were measured within the range from 15 to 60 °C, it was very nicely shown that the constants decreased with increased portion acetonitrile and/or increased temperature (see Fig. 1 in ref. [26]). Thus, interestingly the underlying explanation of the larger retention factor at increased acetonitrile content in the eluent (*cf.* Fig. 1) is the same as the reason for the larger retention factor at a higher column temperature; in both cases the dielectric constant is decreased. Thus, in both cases, the conditions for increased hydrogen bonding are improved.

#### 4.2. Adsorption study at various water/acetonitrile mixtures

To gain a deeper quantitative knowledge about the retention mechanism nonlinear adsorption investigations were performed at different water to acetonitrile ratios in the eluent. To this end, the ECP method, presented in the introduction and in the theoretical section, was used to determine the adsorption isotherms. In particular, separate volume and mass overloaded injections were made of GG and GGG, respectively using as eluent (i) Milli-Q water/acetonitrile (0/10, v/v), (1/9, v/v) and (2/8, v/v). As shown in Fig. 3, two 500- $\mu$ L injections for each solute and eluent composition were performed, GG (Fig. 3a) and GGG (Fig. 3b). A careful examination of the lines for each peptide certified that the system allowed adequate reproducibility, which is required when the profiles are used to generate nonlinear adsorption data. The shapes of the overloaded profiles are "right angular-triangular" (i.e. sharp fronts and diffusive rears) revealing that their corresponding adsorption isotherms are convex (i.e. type I). Convex adsorption isotherms could be determined using the ECP method. However, many different adsorption isotherms models are available even for the more simple type I case [12]. Except for the common Langmuir

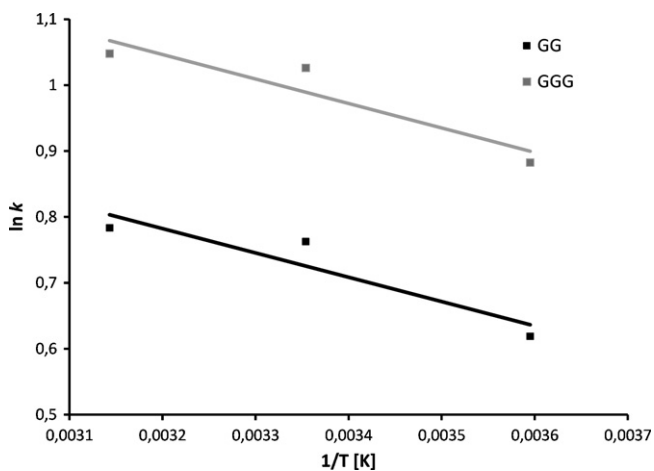


**Fig. 2.** van't Hoff plots for the determination of the enthalpy, entropy and selectivity factors ( $\alpha$ ) of adsorption of GG and GGG using an eluent containing 10% acetonitrile. Symbols, experimental data; lines, best linear fit. The values of  $\Delta H$  and  $\Delta S$  were estimated to be 3.08  $\text{kJ mol}^{-1}$  and 17.2  $\text{J mol}^{-1} \text{K}^{-1}$ , respectively, for GG and 3.09  $\text{kJ mol}^{-1}$  and 19.4  $\text{J mol}^{-1} \text{K}^{-1}$  for GGG, from the slope respective of the intercept of the linear fits. 20  $\mu$ L samples of GG and GGG (0.050 mg/mL of each) were injected at column temperatures of 5, 25 and 45 °C. For other experimental conditions see Section 3.

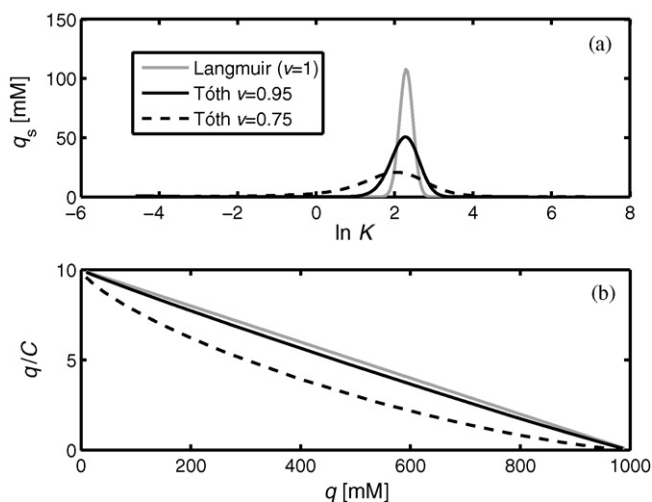


**Fig. 4.** Typical appearance of (a) adsorption energy distributions (AEDs), calculated from synthetic raw data points of a Langmuir (gray line) and two Tóth (black lines) adsorption isotherms and the corresponding (b) Scatchard plots. The Langmuir adsorption isotherm parameters were  $a=K=10$ , and for Tóth  $a=K=10$  where is  $\nu=0.95$  (solid line) for the first model and  $0.75$  (dashed line) for the second model. The number of grid points used in the calculation was 250 and the number of iterations was 100 000.

model there are other one-site models such as the Tóth, Moreau and the Jovanovic models and many of these have been empirically extended as two-site variants. These models describe different and complex adsorption processes such as homogenous or heterogeneous energy distribution, multi-layer adsorption or solute–solute interactions. In order to understand the actual separation process it is therefore of crucial importance to properly evaluate which model most correctly describes the current situation. One must recognize that after model fitting the raw adsorption data are presented as a parameter estimate of the selected model. Thus, if the wrong adsorption model is selected, a wrong adsorption mechanism is assumed.

#### 4.2.1. Evaluation of the adsorption data by Scatchard plots and by adsorption energy distribution calculations

The adsorption was first evaluated using Scatchard plots. Thereafter, the adsorption was characterized by calculating the AED. The combined use of this two-step evaluation procedure, allowed an extensive narrowing down of the number of possible models to be fitted to the adsorption isotherms.

Fig. 4a shows the typical appearance of AEDs, calculated from synthetic raw data points of a Langmuir (gray line) and two Tóth (black lines) adsorption isotherms (according to the procedures described in Section 2.3). One of the Tóth models has  $\nu=0.95$  (solid line) and for the other  $\nu=0.75$  (dashed line). In fact, the Langmuir equation is a Tóth model with  $\nu=1$  (cf. Eqs. (2) and (4)). The Langmuir model has got a quite narrow AED, since its distribution is a Dirac function. The adsorption energy at the apex and the area of the distribution corresponds to the association equilibrium constant ( $K$ ) and the monolayer saturation capacity ( $q_s$ ), respectively. The Tóth model has got a heterogeneous AED that tails toward lower energy. As can be seen from the figure, the smaller the  $\nu$ -value is as compared to 1, the greater the degree of heterogeneity. The more heterogeneous the Tóth adsorption isotherm, the more pronounced is the tailing; this is illustrated by the larger degree of tailing when  $\nu$  is 0.75 (dashed line) as compared to when  $\nu$  is 0.95 (solid line) in Fig. 4a.

Scatchard plots are a useful tool for reduction of possible adsorption models that could describe the separation process. Different

adsorption isotherm models will result in different Scatchard plots. A concave Scatchard plot is true for, e.g. Tóth and  $n$ -Langmuir, convex Scatchard plots are true for, e.g. Jovanovic and Fowler adsorption isotherm models [12], and linear Scatchard plots are only true for the Langmuir adsorption isotherm model. However, the smaller the  $\nu$ -values are as compared to 1 in the Tóth model, the larger the curvature in the Scatchard plot (see Fig. 4b). Unfortunately, the bi-Langmuir model gives a more or less similar shaped Scatchard plot as the Tóth model, especially if the difference between the adsorption energies is small, e.g. phenols adsorption to ODS columns [16]. So from only Scatchard plots it is often hard to distinguish between models having different degrees of heterogeneity. On the other hand, the AED-plot provides an excellent tool to distinguish models with different degrees of heterogeneity but also with different heterogeneous energy distribution [25]. The bi-Langmuir model would produce a bimodal AED, compared to the unimodal solution for Tóth, making AED a powerful companion for model selection. As an example, recently it was found that both the bi-Langmuir and the Tóth models fitted equally well to adsorption isotherms acquired for the adsorption of R-1-indanol to cellulose tribenzoate [27]. Shortly thereafter again the bi-Langmuir model and the Tóth model were indistinguishable, in this case for phenol and caffeine on a Kromasil ODS column [28]. However, that was the time when AED calculations were introduced for HPLC and when applied for the two cases, a clear distinction could be made between the two models [28].

The adsorption isotherms and the corresponding Scatchard plots for the adsorption of (a) GG and (b) GGG, respectively, are shown in Fig. 5. The data were determined at different eluent contents of acetonitrile: 0% (solid lines), 10% (dashed lines) and 20% (gray lines). The Scatchard plots (Fig. 5a<sub>II</sub> and b<sub>II</sub>) are more or less linear at 0% acetonitrile but turn increasingly toward concave non-linearity the larger the fraction acetonitrile in the eluent. In the case of GGG as solute, the degree of nonlinearity is even more pronounced at increasing acetonitrile content (cf. Fig. 5b<sub>II</sub>); here even at 0% acetonitrile there is a slight tendency to nonlinearity close to 0 $q$ . To summarize, the Scatchard plots indicate that a homogeneous Langmuir model could describe the adsorption best when the eluent contains only water (at least for GG) but that a heterogeneous adsorption models like Tóth or bi-Langmuir describe the system best when the eluent contains acetonitrile. However, just from the Scatchard plot which model should be used cannot be confidentially stated.

To further reduce the number of possible models the corresponding AED-plot of the adsorption of the two peptides GG (Fig. 6a) and GGG (Fig. 6b) also has to be examined, and a combined analysis of the two tools has to be made. The AED of GG at 0% acetonitrile in the eluent was found to be unimodal (cf. Fig. 6a black solid line) and with this information all multimodal models could be ruled out at 0% acetonitrile for GG, e.g. bi-Langmuir, bi-Tóth etcetera. The AED of GG at 10% and 20% acetonitrile in the eluent turns successively more to a heterogeneous AED that tails toward lower energy, however, interestingly the energy distribution is still unimodal (cf. Fig. 6a, dashed and gray lines).

The AED of GGG at 0% acetonitrile in the eluent is tailing slightly toward lower energy (cf. Fig. 6b black solid line) indicating that a heterogeneous adsorption model like Tóth describes the system best. This is in contrast to the AED data of GG at 0% acetonitrile where a homogenous energy interaction was indicated. At increasing content acetonitrile in the eluent, the AED-plot of GGG turn successively more to a heterogeneous and even bimodal AED (cf. Fig. 6b, dashed and gray lines). At 20% acetonitrile in the eluent, the AED-plot of GGG clearly comprises of two adsorption sites of different energies of interaction and of different capacities; the higher energy interaction has a smaller capacity, i.e. a smaller area in the AED-plot (cf. Fig. 6b, gray line).

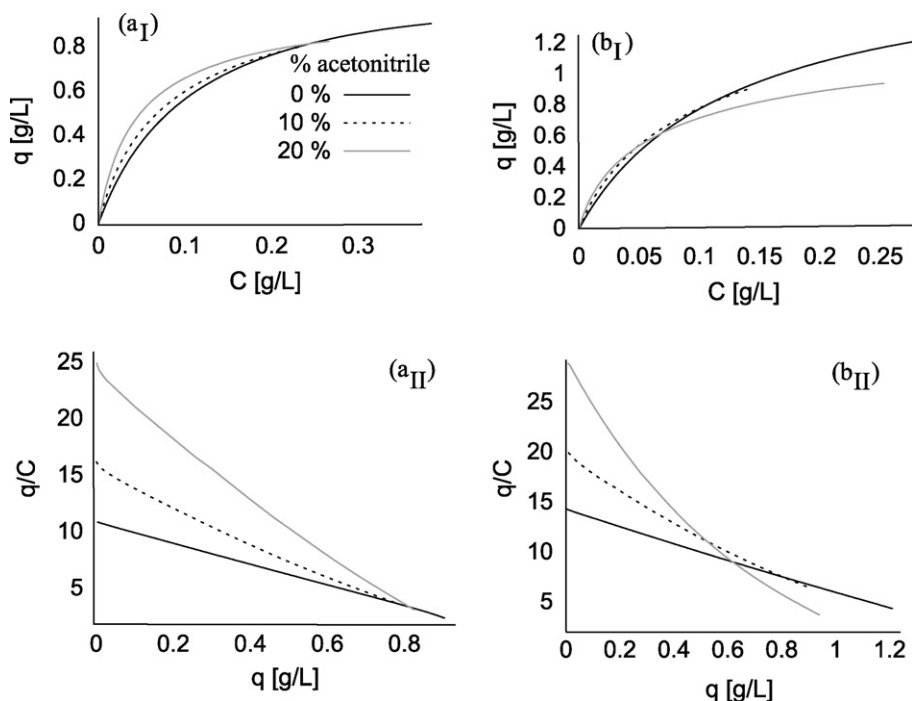


**Fig. 5.** (a–b) The series of sub figures show the (I) adsorption isotherms, (II) the corresponding Scatchard plots for (a) GG and (b) GGG, respectively. The data were determined at different eluent contents of acetonitrile: 0% (black solid lines), 10% (dashed lines) and 20% (gray solid lines). For other experimental conditions see Section 3.

#### 4.2.2. A deeper look at the evaluation tool adsorption energy distribution (AED) calculations

As shown above, the AED of GG at 20% acetonitrile indicated a heterogeneous AED that tails strongly toward lower energy. However, even if the tailing is strong, the energy distribution is still unimodal (cf. Fig. 6a, gray lines). In Fig. 6 the AED was calculated using 200 000 iterations. In Fig. 7 is compared the resulting AED-plots calculated using 200 000 iterations (gray line) and 10 million iterations (black line), respectively. We can see that when the much larger number of iterations are used, the strong tailing toward lower energy distribution turns into a second adsorption site, so that

the whole AED-plots turns bimodal (cf. Fig. 7, black line). Interestingly, the lower energy interaction is the one with the smaller capacity, in contrast to the bimodal case of GGG at 20% acetonitrile (cf. Fig. 6b, gray line). This result indicates that there are “borderline” cases when a heterogeneous unimodal interaction showing a large degree of tailing in reality is a bimodal interaction. Thus, we have to be careful in interpreting AED data and instead combine all information in a holistic way. It should be mentioned, however, that when 10 million iterations were applied for the other experiments in Fig. 6, it did not change the AED-plots in any qualitatively way.

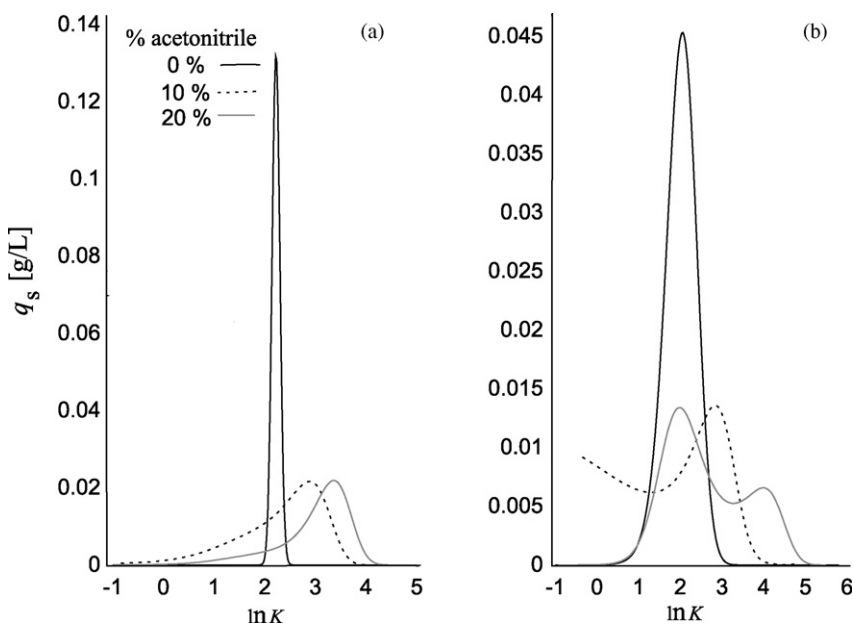


**Fig. 6.** (a–b) The AED calculations for (a) GG and (b) GGG. The data were determined at different eluent contents of acetonitrile: 0% (black solid lines), 10% (dashed lines) and 20% (gray solid lines). The AED were calculated using 300 grid points and using 200 000 iterations. For other experimental conditions see Section 3.

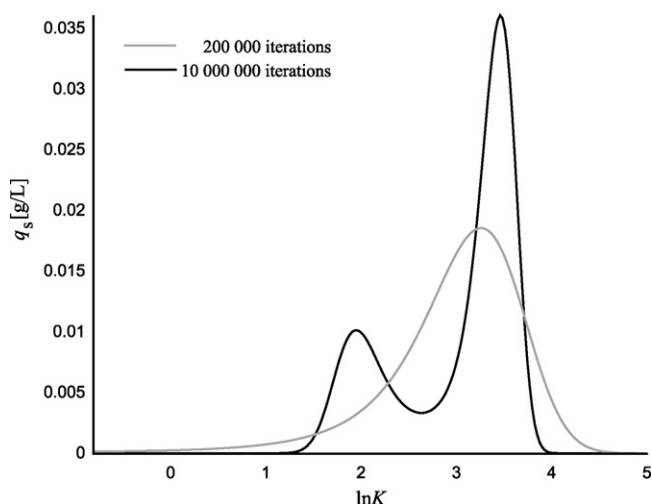


**Fig. 7.** AED calculations for GG at 20% acetonitrile in the eluent using 300 grid points and a number of 200 000 iterations (gray line) and 10 million iterations (black line), respectively. For other experimental conditions see Section 3.

The result in Fig. 7 triggered us to take a deeper look at the ability of the AED-tool to resolve interaction sites of close levels of energy. Heterogeneity around one adsorption can have a completely different physical chemical explanation as compared to heterogeneity caused by two different adsorption sites. The former situation yields an unimodal energy of interaction and can be modeled by using the Tóth model and the latter has a bimodal AED and can simply be modeled for by using the bi-Langmuir model. Both cases, gives a more or less concavely curved Scatchard plot. The more heterogeneous the Tóth adsorption isotherm, the more pronounced is the forward tailing of the AED which is illustrated by the larger degree of tailing when  $\nu$  is 0.75 (dashed line) as compared to when  $\nu$  is 0.95 (solid line), as illustrated in Fig. 4a. From the

series of adsorption isotherms and corresponding Scatchard and AED-plots in Figs. 5 and 6, it is obvious that the adsorption turns from more homogenous to heterogeneous as the acetonitrile concentration in the eluent is increasing. We can see that heterogeneity around one site (described by the Tóth model) in this case, is an intermediate step before the heterogeneity evolves into different sites. We can also see that if the numbers of iterations are not sufficient, heterogeneity because of two sites can falsely be assumed to be heterogeneity around one site.

To understand this phenomenon, a synthetic study was undertaken; a series of AED calculations were made, with different number of iterations, on data from synthetic real bi-Langmuir adsorption isotherms showing different degrees of heterogeneity. The resulting AED-plots are shown in Fig. 8. In this case, there are two sites, one large capacity and main site with also a large energy of interaction; the monolayer capacity,  $q_s$ , is 0.05 g/L and the equilibrium constant, expressed as  $\ln K$ , is 6. But there is also a second site, with more or less lower energy of interaction and with lower monolayer capacity. The calculations show how the AED-plots appear as the second lower energy site, has an energy of interaction going from  $\ln K=5.5$  to  $\ln K=3.5$ . Fig. 8a<sub>I</sub> shows the AED-plots when the monolayer capacity of the low energy site is 10 times smaller than that of the first site and in Fig. 8b<sub>I</sub> it is only 2.5 times smaller; in both cases the number of iterations are 200 000. In the first case, i.e. low energy site has a 10 times lower capacity, it is only possible to recognize a site with a much lower energy of interaction ( $\ln K=3.5$  in Fig. 8a<sub>I</sub>) as compared to a high energy site. When the low energy site has a somewhat larger capacity, in this case only 2.5 times smaller capacity, a low energy site somewhat closer to the high energy site can be visualized (cf.  $\ln K=4$  in Fig. 8a<sub>I</sub>); However, a difference of  $2\Delta \ln$  units is still required. Even in this case a low energy site of  $\ln K=5$  cannot be resolved from the reference site ( $\ln K=6$ ), instead the AED tails toward lower energy indicating (falsely) heterogeneity around one site (gray dotted line in Fig. 8b<sub>I</sub>). The right figures (Fig. 8a<sub>II</sub> and 8b<sub>II</sub>) show what happens

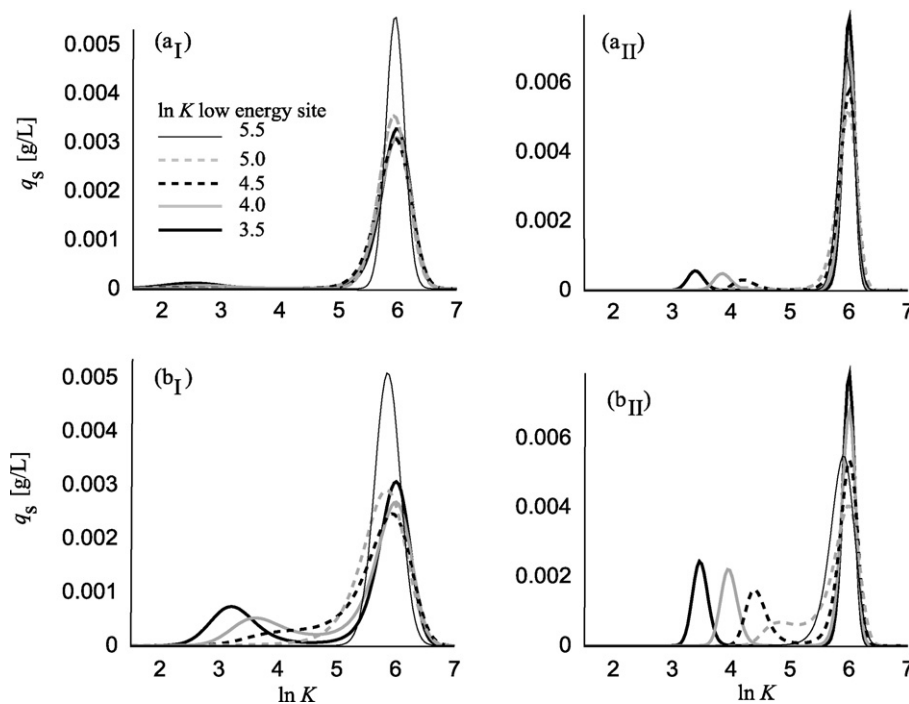


**Fig. 8.** The series of subplot showing the AED calculations for synthetic different bi-Langmuir adsorption isotherms with different levels of low energy sites (a) and (b) solved with different amount of iterations (I) 200 000 and (II) 10 million. The constant high energy site has  $q_s$  of 0.05 g/L and an equilibrium constant of 403.4 L/g corresponding to  $\ln K=6$ . The low energy sites equilibrium constant varies between 33.1 and 244.7 L/g corresponding to  $\ln K$  between 3.5 and 5.5. The capacity for the low energy site: (a) 0.005 g/L and (b) 0.02 g/L. The AEDs were calculated using 300 grid points.



**Table 3**  
Adsorption data fitted to bi-Langmuir and Tóth adsorption isotherm model.

Solute	% acetonitrile	$a_1$	$K_1$ (1/M)	$a_2$	$K_2$ (1/M)	$\nu$	$q_{s1}$ (mM)	$q_{s2}$ (mM)
GG	0	10.89	1228	NA	NA	1.00	8.87	NA
GG	10	16.24	1879	NA	NA	0.85	8.64	NA
GG	20	3.92	1307	20.20	4472	NA	3.00	4.52
GGG	0	14.38	1501	NA	NA	0.96	9.58	NA
GGG	10	4.90	885.9	14.69	4375	NA	5.53	3.36
GGG	20	7.10	1579	21.65	10644	NA	4.50	2.03

to the AED-plots when the numbers of iterations are increased to 10 million; the unimodal interaction turns to a bimodal pattern (site gray dotted lines in Fig. 8b<sub>I</sub> and 8b<sub>II</sub>). However, even with 10 million iterations, it is not possible to reveal a bimodal pattern through AED calculations when the low energy site has a closer energy of interaction ( $\ln K=5.5$ ) relative the reference site ( $\ln K=6$ ).

A similar pattern was found when the second site had energy of interaction that is stronger than the reference site, i.e. in this case  $\ln K$  was going from 6.5 to 8.5 (unpublished results).

#### 4.2.3. Fitting of proper models describing the adsorption process

The AED calculations of the adsorption of GG at 0% acetonitrile in the eluent (cf. Fig. 6a) indicates that a Langmuir model should fit well to the adsorption isotherm at 0% acetonitrile which is also indicated by the more or less linear Scatchard plot (cf. Fig. 5a<sub>II</sub>). The Scatchard plots of GG at increasing acetonitrile in the eluent indicate heterogeneity; The AED-plots complement this picture and adds the information that at 10% acetonitrile the heterogeneity is unimodal and at 20% acetonitrile bimodal.

Consequently, and as can be seen from Table 3 presenting the best adsorption models and their parameters, the Langmuir model was best for GG at 0% acetonitrile in the eluent. For GG at 10% acetonitrile in the eluent, the Tóth model was found to be significantly better (95%, *F*-test) than Langmuir with  $\nu$  the parameter at 0.85 indicating a certain degree of tailing (cf. Table 3). In the case of 20% acetonitrile in the eluent, the bi-Langmuir model was best (cf. Table 3) as indicated by the AED-plot. As mentioned above, the AED calculation with the larger number of iterations for GG at 20% acetonitrile showed a bimodal energy of interaction, typical for the bi-Langmuir model, see the black line in Fig. 7.

In the case of GGG, all Scatchard plots show a deviation from linearity and the AED-plots confirms the heterogeneity but specify also that it revolves around one site at 0% acetonitrile in the eluent and comprises of two sites at 10 and 20% acetonitrile in the eluent. Thus, the raw adsorption data of GGG at 0% acetonitrile in the eluent were fitted to both the Langmuir and the Tóth models. The Tóth model was found to be significantly better (95%, *F*-test) than Langmuir with a value of 0.96 for the  $\nu$  parameter indicating a very slight degree of tailing (see Table 3). This is in agreement with the barely observable degree of nonlinearity of the corresponding Scatchard plot. In the case of 10% and 20% acetonitrile in the eluent, the bi-Langmuir model best described the adsorption of GGG (cf. Table 3) as indicated by the corresponding AED-plots (cf. Fig. 6b).

The compositions of the fitted parameters presented in Table 3 describe perfectly the corresponding parameters that can be derived from the AED-plots. Note also that, the AED of the bimodal interaction of GG at 20% acetonitrile shows that the site with the larger energy of interaction (site 2, at right in the AED in Fig. 7 black line) has a higher capacity than the site with the lower energy of interaction (site 1, at the left in the AED in Fig. 7) while the opposite is the case for GGG at the same acetonitrile content (cf. Fig. 6b). The same pattern can be read in Table 3 at 20% acetonitrile in the eluent; for GG  $q_{s1} = 3.00$  and  $q_{s2} = 4.52$  mM while for GGG  $q_{s1} = 4.50$  mM and  $q_{s2} = 2.03$  mM.

It was recently found that an error in the hold-up volume can result in the assumption of wrong adsorption mechanisms [23,29]. A complete synthetic investigation of this phenomenon was made, showing that for a true Langmuir an underestimated hold-up time could lead to a more heterogeneous model such as Tóth or bi-Langmuir. For overestimated hold-up times a true Langmuir model fits better to models describing multi-layer adsorption or solute–solute interactions such as Jovanovic and Moreau [29]. But in our case, we can confidently state that we have a slightly overestimated hold-up time; since the hold-up marker has a slightly higher retention volume than the solutes at high urea concentrations (see Table 2). Thus, a wrong assumption about the Tóth model because of an error in the hold-up volume can be completely eliminated.

#### 4.3. Putative separation mechanism

As demonstrated above, there are clear indications that the adsorption is due both to hydrogen bonding and to electrostatic interactions. According to the manufacture, the amount of negatively charged groups (sulphate and carboxyl) in Superose 12 10/300 GL is within the range 1–2  $\mu\text{mol/mL}$  gel [30]. This amount corresponds to monolayer saturation capacity ( $q_s$ ) values between 8 and 16 mM which are in a similar magnitude as the determined saturation capacity (cf. Table 3). This requires that there is a 1:1 stoichiometry at the adsorption site, which is a good assumption due to the fact that GG and GGG have similar monolayer saturation capacities (cf. Table 3). To further investigate if the interaction can be charged, pH was measured in the samples for GG and GGG at concentrations between 0 and 5 g/L solved in Milli-Q water and in eluent (9/1 water/acetonitrile solution (v/v)), respectively. The pH of GG and GGG varied between 4.7 and 5.3 in the water solutions and between 5.0 and 5.2 in the eluent solutions. The isoelectric point (*pI*) was identical for GG and GGG and was calculated to 5.52 [31] which clearly indicates that both the amine and the carboxyl groups are charged.

Thus, many facts argue towards electrostatic interactions: (i) the peptides are charged (ii) a higher acetonitrile content in the eluent results in larger peptide retentions as demonstrated in Fig. 1 (iii) sodium chloride added to the eluent decreases efficiency the peptide retentions. In addition (iv), the capacity terms estimated from the adsorption study are of similar magnitude as compared to the manufacturers information about number of charged groups on the gel. These facts and especially the last one (point iv) strongly indicate that electrostatic interactions provides a major mechanism behind the peptide adsorption.

On the other hand, hydrogen bond formations cannot be ruled out. Point (ii) above, that the retention of the peptides decrease with increasing acetonitrile content in the eluent, can also be equally well interpreted as caused by hydrogen bond formations. In addition, the endothermic adsorption behaviors revealed in the temperature study, strengthen the hypothesis of polar interactions, by hydrogen bonding. Thus, the explanation of the larger retention factor at increased acetonitrile content in the eluent (cf. Fig. 1) is the same as the reason for the larger retention factor at a higher column temperature; in both cases the dielectric constant is decreased

[26]. Thus, in both cases, the conditions for increased hydrogen bonding are improved. In addition, the effects of adding urea (*cf.* Table 2) points in the same direction. In fact, the urea result contradicts the electrostatic explanation because urea should not affect electrostatic interactions. Moreover, the fact that GGG is consistently more retained than GG (*cf.* Fig. 2) cannot be explained by electrostatic interactions since GG and GGG are more or less identically charged. On the other hand, GGG has a further possibility for hydrogen formations through the extra amid group in the peptide bond link, which can explain its larger retention volume as based on hydrogen formation.

## 5. Conclusion

There is today an increased interest in the use of polar stationary phases combined with partly aqueous eluents for the separation and analysis of polar low molecular weight solutes, e.g. peptides. In this paper the highly cross-linked 12% agarose gel Superose 12 10/300 GL gel is introduced as an alternative media for hydrophilic interaction chromatography using simple peptides as model solutes. The focus of the study is on the adsorption mechanism. A previous investigation using polyphenols as solutes on the same gel, revealed that the retention could be explained by a mixed – hydrophobic and – hydrogen bond formation mode [4].

Firstly, an analytical study was made, aimed at determining the relation between the retention of the model peptides (GG and GGG) and the acetonitrile content. The retention time increased with increasing acetonitrile content in the eluent, demonstrating that polar binding prevails in this phase system. Further studies were made with urea and sodium chloride added to the eluent. At 2 M urea added to the eluent, GG and GGG eluted at a combined elution volume below the determined hold-up volume. Urea added to the eluent should not affect electrostatic interactions; therefore it was concluded that hydrogen bond formation contributes to the retention. On the other hand, both peptides were eluted after one void volume at low concentrations of sodium chloride, indicating that electrostatic interactions play a major role for the peptide retention as well. This is also in line with the fact that the peptides are zwitterions at the actual eluent pH. A temperature investigation of analytical retention data showed that both GG and GGG were adsorbed through an endothermic behavior with positive enthalpies and entropies of adsorption. The values of  $\Delta H$  and  $\Delta S$  were estimated to  $3.08 \text{ kJ mol}^{-1}$  and  $17.2 \text{ J mol}^{-1} \text{ K}^{-1}$ , respectively, for GG and  $3.09 \text{ kJ mol}^{-1}$  and  $19.4 \text{ J mol}^{-1} \text{ K}^{-1}$  for GGG, from the slope respective the intercept of the linear fits. The similar  $\Delta H$  values make it impossible to use the temperature to change the selectivity. The larger entropy factor for GGG as compared to GG is probably because GGG occupies a larger fraction of the surface making the degree of displacement of ordered water molecules larger [32].

Secondly, adsorption isotherms for GG and GGG were determined at different acetonitrile content in the mobile phase, going from 0% to 20%, using the elution by characteristic point method combined with a new evaluation approach, the calculation of the AED. By calculating the AED of the interaction, we could narrow down the possible number of adsorption isotherm models, prior to the selection of a proper interaction model to fit to the data. The tools Scatchard plots and AED as well as the fitting of proper models

describing the adsorption processes, all showed that the unimodal homogenous (Langmuir) or mildly heterogenous interaction (Tóth model) turns into more pronounced heterogeneous interactions comprising of two different interaction sites (bi-Langmuir) when going from 0% to 20% acetonitrile content in the eluent.

Thus, the nonlinear adsorption study confirmed the heterogeneity; the larger the content of acetonitrile, the larger the degree of heterogeneity. Thus, a second polar (or perhaps electrostatic) site is evolved as the eluent becomes more and more non-polar; a more non-polar eluent enhances the formation of polar interactions. In this particular case, all analytical runs were made using 10% acetonitrile in the eluent, a situation where a second polar site has just started to be involved as well. Thus we have a mild mixed-mode interaction, where one of the sites is due to hydrogen bond formation and the other probably due to electrostatic interactions.

## Acknowledgements

The authors are grateful for the support given by the National Natural Science Foundation of China (20606032, 20636010, 50773083) and by a grant from the Swedish Research Council (VR).

## References

- [1] A.C. Haglund, J. Chromatogr. 156 (1978) 317.
- [2] US Patent 4,665,164 (1987).
- [3] T. Andersson, M. Carlsson, L. Hagel, P.-A. Pernemalm, J.-C. Janson, J. Chromatogr. 326 (1985) 33.
- [4] J. Xu, T. Tan, J.-C. Janson, J. Chromatogr. A 1137 (2006) 49.
- [5] M. Gu, Z.-G. Su, J.-C. Janson, Chromatographia 64 (2006) 247.
- [6] M. Gu, Z.-G. Su, J.-C. Janson, Chromatographia 64 (2006) 701.
- [7] J. Xu, T. Tan, J.-C. Janson, J. Chromatogr. A 1169 (1–2) (2007) 235.
- [8] M. Gu, Z.-G. Su, J.-C. Janson, J. Chromatogr. Sci. 46 (2008) 165.
- [9] A.J. Alpert, J. Chromatogr. 499 (1990) 177.
- [10] P. Hemström, K. Irgum, J. Sep. Sci. 29 (2006) 1784.
- [11] The whole issue of Journal of Separation Science, vol. 31, no. 9, May 2008, is dedicated to reports dealing with varying aspects on HILIC.
- [12] G. Guiochon, A. Felinger, D.G. Shirazi, A.M. Katti, Fundamentals of Preparative and Nonlinear Chromatography, second edition, Academic Press, Netherlands, 2006.
- [13] A.J. Seidel-Morgenstern, J. Chromatogr. A 1037 (2004) 255.
- [14] T. Fornstedt, P. Sajonz, G. Guiochon, J. Am. Chem. Soc. 119 (1979) 1254.
- [15] M. Vitha, P.W. Carr, J. Chromatogr. A 1126 (2006) 146.
- [16] F. Gritti, G. Guiochon, J. Chromatogr. A 1099 (2005) 1.
- [17] G. Götmar, J. Samuelsson, A. Karlsson, T. Fornstedt, J. Chromatogr. A 1156 (2007) 3.
- [18] H. Guan, B.J. Stanley, G. Guiochon, J. Chromatogr. A 659 (1994) 27.
- [19] L. Raval, T. Fornstedt, J. Chromatogr. A 908 (2001) 111.
- [20] I. Langmuir, J. Am. Chem. Soc. 38 (1916) 2221.
- [21] G. Götmar, R.N. Albareda, T. Fornstedt, Anal. Chem. 74 (2002) 2950.
- [22] J. Samuelsson, A. Franz, B.J. Stanley, T. Fornstedt, J. Chromatogr. A 1163 (2007) 177.
- [23] J. Samuelsson, J. Zang, A. Murunga, T. Fornstedt, P. Sajonz, J. Chromatogr. A 1194 (2008) 205.
- [24] B.J. Stanley, J. Krance, J. Chromatogr. A 1011 (2003) 11.
- [25] B.J. Stanley, G. Guiochon, J. Phys. Chem. 97 (1993) 8098.
- [26] L.G. Gagliardi, C.B. Castells, C. Ràfols, M. Rosés, E. Bosch, J. Chem. Eng. Data 52 (2007) 1103.
- [27] D. Zhou, D.E. Cherrak, K. Kaczamarski, A. Cavazzini, G. Guiochon, Chem. Eng. Sci. 58 (2003) 3257.
- [28] F. Gritti, G. Götmar, B.J. Stanley, G. Guiochon, J. Chromatogr. A 988 (2003) 185.
- [29] J. Samuelsson, P. Sajonz, T. Fornstedt, J. Chromatogr. A 1189 (2008) 19.
- [30] Personal communication: Dr. Bo-Lennart Johansson, R&D Department, GE Healthcare Bio-Sciences, Uppsala, Sweden.
- [31] <http://www.expasy.ch/tools/pi.tool.html>.
- [32] S. Lewin, Displacement of Water and its Control of Biochemical Reactions, Academic Press, London and New York, 1974.